

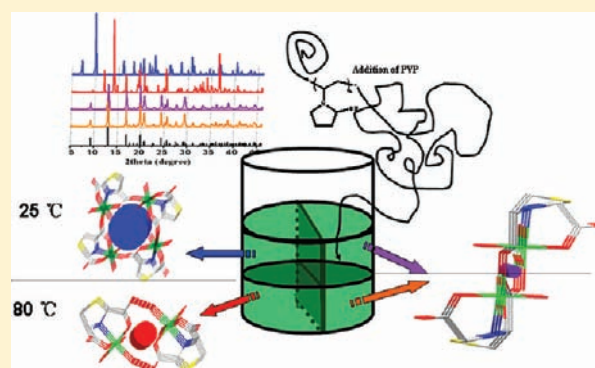
# Chiral Ni(II) Coordination Polymers: Structure-Driven Effects of Temperature and Polyvinylpyrrolidone

Yan-Yan Yin, Jian-Gong Ma, Zheng Niu, Xiao-Chang Cao, Wei Shi, and Peng Cheng\*

Department of Chemistry and Key Laboratory of Advanced Energy Materials Chemistry (MOE), Nankai University, Tianjin 300071, China

## Supporting Information

**ABSTRACT:** Chiral Ni(II) coordination compounds with structures of  $[\text{NiL}(\text{H}_2\text{O})_3]$  (**1**) and  $\{[\text{NiL}(\text{H}_2\text{O})]\cdot 0.5\text{H}_2\text{O}\}_n$  (**2**) ( $\text{H}_2\text{L}$  = thiazolidine 2,4-dicarbonyl acid) have been successfully synthesized by the reaction of  $\text{Ni}(\text{CH}_3\text{COO})_2\cdot 4\text{H}_2\text{O}$  and  $\text{H}_2\text{L}$  in aqueous solution at 25 and 80 °C, respectively. From the same procedure with polyvinylpyrrolidone (PVP) as a surfactant, another corresponding micrometer-scale Ni(II) coordination polymer,  $\{[\text{NiL}(\text{H}_2\text{O})_2]\cdot \text{H}_2\text{O}\}_n$  (**3**), has been obtained at both 25 and 80 °C, which shows a different structure (one-dimensional, 1D) than both **1** (discrete molecule) and **2** (3D). The conversions of structures and conformations are directed by temperature and surfactant (PVP), as confirmed by powder and single-crystal X-ray diffraction. Circular Dichroism (CD) and Second Harmonic Generation (SHG) measurements of the products have been investigated as well, which indicate the potential applications of these products in chiral and nonlinear optical (NLO) areas.



## INTRODUCTION

Research on chiral and helical structures has become more and more important for their essential role in biological functional systems as well as for their unique properties in the areas of photochemistry, chiral recognition, and catalysis.<sup>1</sup> There are mainly two methods to synthesize helical and chiral coordination compounds: one is using a chiral component as the primary linker or supplementary to the “design” of a chiral solid,<sup>2</sup> which demands the component to be chirally pure and stable under the synthesis conditions without racemization.<sup>3</sup> Another method is based on the achiral ligands with spontaneous resolution without any other chiral auxiliaries, and chirality can be introduced into the final product through an external directing force such as solvent and additives.<sup>4,5</sup> In recent years, extensive efforts on these projects led to a huge number of coordination compounds with chirality and initiated a rational design strategy to construct helical and homechiral materials with specific structures and tunable conformations for corresponding applications.<sup>6–10</sup> It has been reported that the addition of surfactants can lead to new coordination and hydrogen bonding interactions with/among metal ions, ligands, and solvents as well as changes of local environment for the whole reaction system,<sup>10,11</sup> which are important for introducing and/or controlling the chirality of the products.<sup>9</sup>

Recently, we reported<sup>12</sup> two Co(II) complexes which go through form conversions (from bulk to nano crystals) together with the exchange of molecular configurations ruled by temperature and the surfactant polyvinylpyrrolidone (PVP). In this study, we will report two new chiral Ni(II) coordination

compounds which exhibit different kinds of form and structure conversions directed by temperature and PVP as well. Through the microemulsion method with PVP as a surfactant, forms of both complexes are converted from bulk crystals to micrometer-scale coordination particles, and during this period molecular structures of both complexes are changed to a totally different one. Nonlinear optical (NLO) properties and obvious Cotton effects in circular dichroism (CD) spectra are observed for these complexes, from which potential application on multifunctional molecular materials could be expected.

## RESULTS AND DISCUSSION

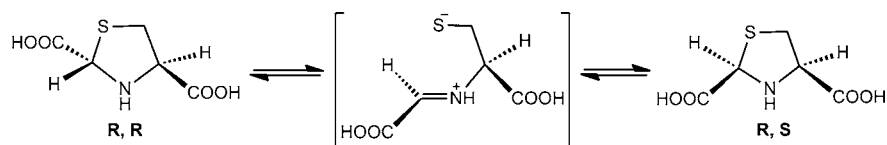
### Synthesis of Bulk and Micrometer-Scale Crystals.

Ligand  $\text{H}_2\text{L}$  ( $\text{H}_2\text{L}$  = thiazolidine 2,4-dicarbonyl acid) was designed to coordinate to metal ions via the nitrogen atom of the heterocycle and the oxygen atoms of the 2,5-dicarboxylate groups. The synthesis of  $\text{H}_2\text{L}$  is simple and in high yield according to the literature method.<sup>13</sup> Although the product contains enantiomers of both (R,R) and (R,S), which are difficult to separate, the expected coordination mode and the reversible conversion (Scheme 1) of the isomers guarantee the enantiomerically pure complexes.<sup>13</sup>

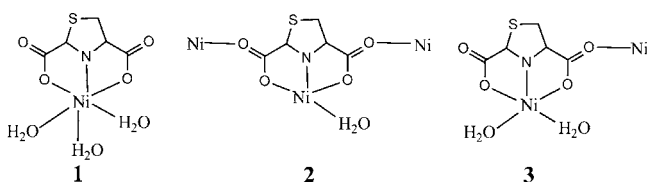
Two Ni(II) complexes with structures of discrete molecule  $[\text{NiL}(\text{H}_2\text{O})_3]$  (**1**) and three-dimensional (3D)  $\{[\text{NiL}(\text{H}_2\text{O})]\cdot 0.5\text{H}_2\text{O}\}_n$  (**2**) were prepared by stirring the mixture of  $\text{H}_2\text{L}$  and  $\text{Ni}(\text{CH}_3\text{COO})_2\cdot 4\text{H}_2\text{O}$  in the aqueous solution at 25

Received: January 16, 2012

Published: March 29, 2012

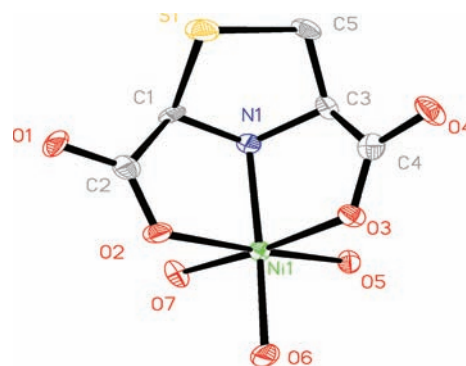
Scheme 1. Conformation Conversion between the Enantiomers (R,S) and (R,R) of H<sub>2</sub>L in Aqueous Solution

and 80 °C for 2 h, respectively. When mixing H<sub>2</sub>L and Ni(CH<sub>3</sub>COO)<sub>2</sub>·4H<sub>2</sub>O in the aqueous solution in the presence of PVP as a surfactant, micrometer-scale coordination particles with the structure of 1D  $\{[\text{NiL}(\text{H}_2\text{O})_2] \cdot \text{H}_2\text{O}\}_n$  (**3**) were obtained at both 25 and 80 °C, respectively. The conformations of the units for these products, the whole synthesis procedure, and the structures of **1–3** are illustrated in Schemes 2 and 3, respectively.

Scheme 2. The Conformations of the Units for **1–3**

**Structural Analysis.** *Structure of  $[\text{NiL}(\text{H}_2\text{O})_3]$  (**1**).* The atomic numbering scheme and atom connectivity for **1** are shown in Figure 1. **1** crystallizes in the orthorhombic system with chiral space group  $P2_12_12_1$ . The structure of **1** features a discrete molecule with the ligand L in a  $\mu_1$ -bridging mode. The Ni(II) ion is coordinated by L via the nitrogen atom of the heterocycle and oxygen atoms of the 2,5-dicarboxylate groups forming two fused five-membered rings (Ni–O(2) = 2.040(2) Å, Ni–O(3) = 2.038(3) Å, and Ni–N(1) = 2.107(2) Å). Three oxygen atoms from water molecules are coordinated to Ni(II) with Ni–O distances in the range of 2.029–2.076 Å to complete the octahedral coordination sphere of the Ni(II) ion in one unit.

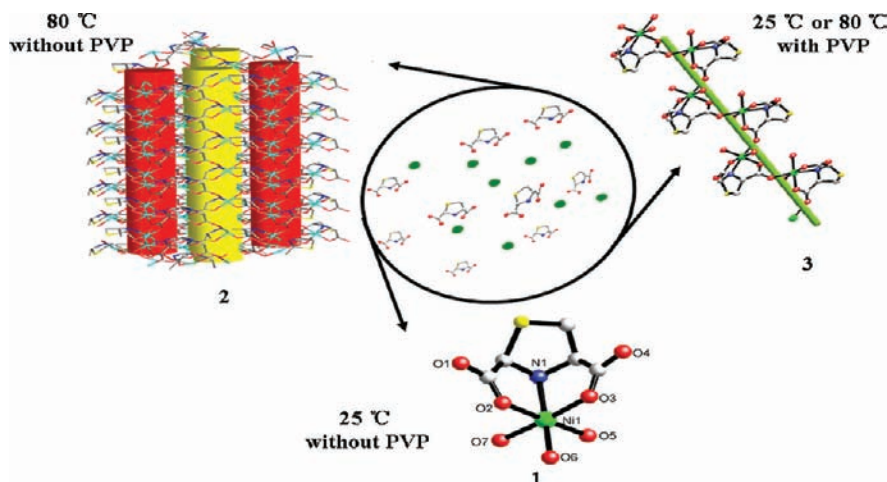
The adjacent  $[\text{NiL}]$  units are connected together through strong hydrogen bonding interactions ( $\text{O} \cdots \text{O} = 2.764$  Å) between terminal water molecules (O6) and carboxylic oxygen atoms (O1) to form a 1D left-handed helical chain (Figure 2a,



**Figure 1.** Perspective view of coordination environments of the Ni(II) ion and the coordination mode of L<sup>2-</sup> in **1** (hydrogen atoms are omitted for clarity).

surrounding the blue column) that spirals down the crystallographic *a* axis with a width of ca. 4.715 Å and a pitch of ca. 5.824 Å. This Ni(II) chain is connected with the other four adjacent chains (left handed) through the hydrogen bonding interactions between the carboxylic oxygen atom (O1) and terminal water molecule (O5) ( $\text{O} \cdots \text{O} = 2.774$  Å), associated with the formation of a right-handed helical chain as shown in Figure 2a (surrounding the purple column). A 3D supramolecular network is formed by both hydrogen-bonding and coordinating interactions as shown in Figure 2a. The topology structure can be represented as a (10,3)- $\alpha$ -connected net by simplifying the carboxylic oxygen O4 and Ni(II) site as a three-connected node (Figure 2b). The Schläfli symbol of this three-nodal (10,3)-connected net is  $(6^3)(6^{12},8^3)$ .

*Structure of  $[\text{NiL}(\text{H}_2\text{O})] \cdot 0.5\text{H}_2\text{O}$  (**2**).* In the structure of **2**, the ligand L adopts a  $\mu_3$ -bridging mode and coordinates to the Ni(II) center by one nitrogen atom and two oxygen atoms to form two fused five-membered rings (Ni–O(2) = 2.028(2) Å,

Scheme 3. Schematic Representation of the Generation of Discrete **1**, 3D Framework **2**, and 1D Left Helical Chain **3** Triggered by Temperature or PVP

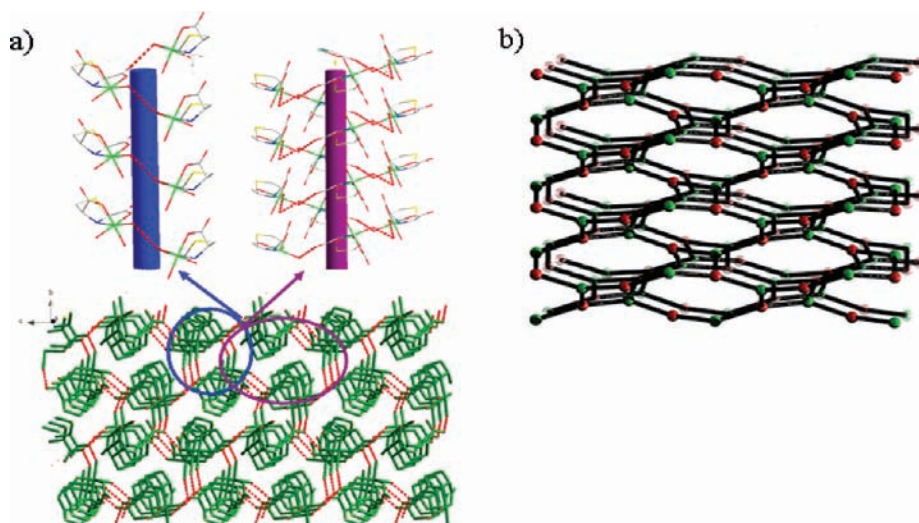


**Figure 2.** (a) View of the 3D supermolecular network constructed from 1D helical chains by hydrogen bonds along the  $c$  axis in **1**. (b) Topological structure of **1**.

Ni–O(3) = 2.064(2) Å, and Ni–N(1) = 2.096(2) Å; Figure 3). Two carboxylic oxygen atoms (O4A and O1B) from the other

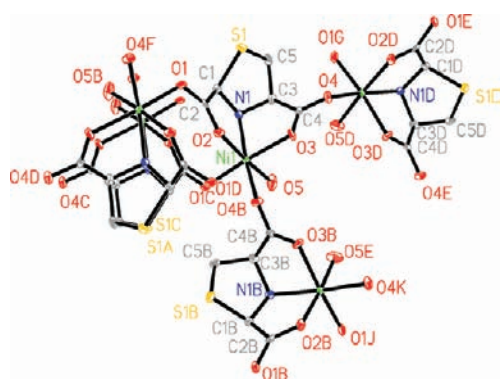


**Figure 3.** Perspective view of coordination environments of the Ni(II) ion and the coordination mode of the  $L^{2-}$  ligand in **2** (hydrogen atoms are omitted for clarity).

two ligands coordinate to the Ni(II) ion with distances of Ni–O(1) = 2.065(2) Å and Ni–O(4) = 2.089(2) Å, respectively. A water molecule coordinates to Ni(II) with a distance of 2.039(3) Å to complete the octahedral coordination sphere of the Ni(II) ion in one unit. Both carboxylate groups of the ligand exhibit the  $\mu_2$ -bridging coordination mode.

In **2**, neighboring Ni(II) ions are connected to each other through carboxylate groups to form two kinds of channels with an approximate cross-section of  $8.32 \times 5.91$  Å and  $13.04 \times 5.59$  Å, as shown in Figure 4a. One of the channels (red column) is formed by a right-handed helical chain, which is constructed by the metal center and one carboxylate group. This channel is filled with numerous coordinated and lattice water molecules, so that it can be considered a “hydrophilic” channel. The other kind of channel (yellow column) is formed by triple-stranded left-handed helical chains, which are linked by the Ni(II) ions and the other carboxylate groups. This channel is filled with the organic ligand (heterocycle) yet without any lattice water or coordination water inside, which can be considered a “hydrophobic” one. When considering Ni(II) ions as four-connected nodes, each node is coordinated with four  $\mu_3$ -L

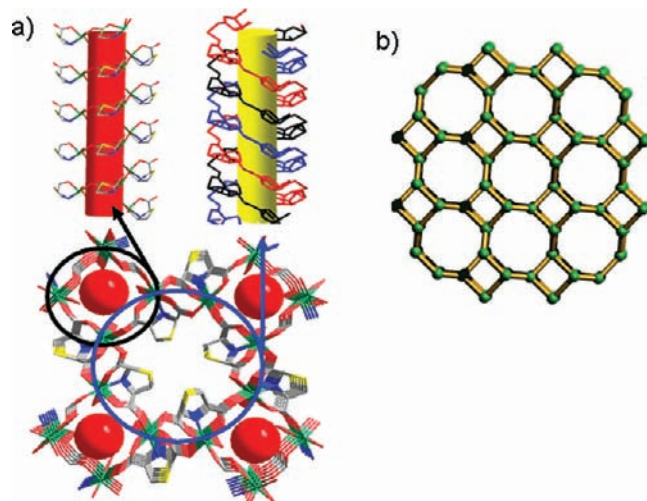


**Figure 4.** (a) View of the 3D supermolecular network constructed by 3-fold right-handed (surrounding red column and forming the hydrophilic channel) and 1D left-handed (surrounding yellow column and forming the hydrophobic channel) helical chains along the  $c$  axis in **2**. (b) The topological structure of **2**.

ligands, and noninterpenetrating (10,3)- $\alpha$  nets are observed, which is a well-known topology of the  $SrSi_2$ -type structure (Figure 4b).<sup>14</sup> The Schläfli symbol of this three-nodal (10,3)-connected net is  $(6^{12}.8^3)$ .

**Characterization of Hierarchical Microspheres.** The phase and crystallographic structure of product **3** on the micrometer scale are determined by powder X-ray diffraction (PXRD), shown in Figure 5. The microparticles obtained through the microemulsion method with PVP at 25 and 80 °C show different PXRD patterns from that of **1** and **2** (Figure 5). Single crystals of **3** in the bulk form are obtained by recrystallization of the nanoparticles from the water/methanol solution (see the Experimental Section), whose structure has been confirmed to be the same as the micrometer particles of **3** by PXRD, as shown in Figure 5. The strong and sharp diffraction peaks in the PXRD pattern for the micrometer particles of **3** indicate that the product is well crystallized. All of the peaks are well in accordance with that in the simulated



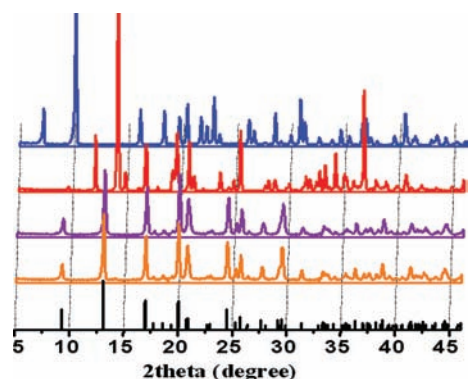


**Figure 5.** PXRD patterns of **1** (red) and **2** (blue) as well as the micrometer particles of **3** obtained at 25 (orange) and 80 °C (violet). The black line is the simulated PXRD pattern from single crystal X-ray diffraction data of **3** in the bulk crystal form.

pattern based on the single crystal structure without any other impurities. The differences between the two kinds of reaction systems (with and without PVP) confirm the important structure-induction effects of PVP as a surfactant.

According to the single-crystal X-ray diffraction data, the coordination environment of **3** is shown in Figure 6. The

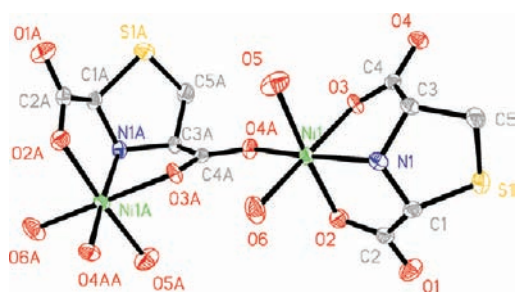


**Figure 6.** Perspective view of coordination environments of Ni(II) ions and coordination modes of ligand L in **3** (hydrogen atoms are omitted for clarity).

structure of **3** features a 1D helical chain with the ligand L in a  $\eta^2$ -bridging mode. The Ni(II) ion is octahedrally coordinated by one nitrogen atom and two oxygen atoms from a single ligand to form two fused five-membered rings (Ni–O(2) = 2.019(2) Å, Ni–O(3) = 2.069(2) Å, and Ni–N(1) = 2.054(2) Å). One carboxylate oxygen atom (O4A) from another ligand and two water molecules coordinate to the Ni(II) ion to complete the octahedral coordination sphere (Ni–O(4A) = 2.061(2) Å, Ni–O(5) = 2.077(2) Å, and Ni–O(6) = 2.060(2) Å). One kind of carboxylate group exhibits a  $\mu_2$ -bridging mode and connects Ni(II) sites into a left-handed helical chain along the *b* axis. The adjacent Ni(II) chains are connected to each other by strong hydrogen bonds among carboxylic oxygen atoms, coordinated water molecules, and lattice water molecules (O1...O7 = 2.726 Å and O6...O7 = 2.764 Å) to form a supramolecular network (Figure 7).

The morphologies of **3** as a micrometer-scale coordination polymer prepared at 25 and 80 °C are shown in Figure 8. The panoramic SEM image in Figure 8a shows that the product obtained at 25 °C is dispersed microspheres with diameters of ~10–12  $\mu\text{m}$ . A typical microsphere is shown in the magnified SEM image in Figure 8b, which is assembled by belt-shaped microstructures. More details of these belt-shaped structures with smooth surfaces can be observed in Figure 8c, which are

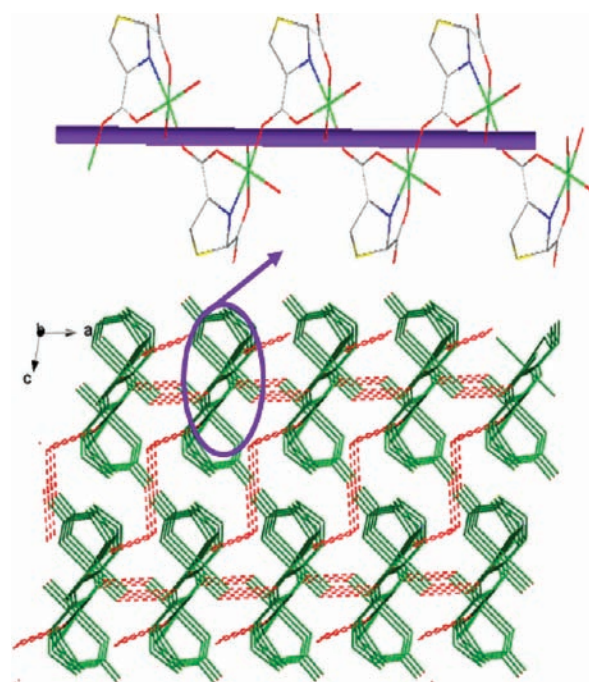


**Figure 7.** View of the 3D supermolecular network constructed from the 1D left-handed helical chain by hydrogen bonds along the *b* axis in **3**.

about 1  $\mu\text{m}$  in width, 3.5  $\mu\text{m}$  in length, and 450 nm in thickness. The morphology of the product obtained at 80 °C is almost the same, although some microspheres are broken into small pieces (Figure 8d). Details of these hierarchical microspheres, which are assembled by micrometer belts with a width of ~2  $\mu\text{m}$  and diameter of ~110 nm, are shown in Figure 8e and f.

**Structure Switched by Temperature and Directed by PVP.** In all of the structures **1**–**3**, each Ni(II) ion adopts an octahedral geometry and coordinates with the ligand in a ratio of 1:1 to afford the helical chain. Water molecules, which play an important role in forming the hydrogen bonding architecture, bind to the metal center to saturate the whole coordination number of Ni(II) ions. An important character in the structures of both **1** and **3** is the hydrogen bonding interactions between carboxylic oxygen atoms and coordinated or lattice water molecules which link the [NiL] units (in **1**) or the [NiL]<sub>n</sub> chains (in **3**) to form 3D structures. When these water molecules are removed by extra stimuli (e.g., the adjustment of the temperature or the addition of PVP), carboxylic oxygen atoms take the place of water molecules to coordinate in the free sites of Ni(II) of the neighbor unit, which leads to 1D or 3D polymer structures, as shown in Scheme 4.

The hydrogen-bonded network in **1** provides favorable conditions for the structure conversion. The geometric proximity between Ni(II) ions and the carboxylic oxygen atoms from adjacent units in **1** is maintained by OH...O hydrogen bonding. Since thermal dehydration can remove water molecules of the structure to form higher dimensionality,<sup>15</sup> upon gentle heating of the reaction system, **1** could release water molecules accompanied by the formation of new Ni–O bonds with a carboxylate group, and the 3D network of **2** can be formed. The structure of **3** was obtained through the microemulsion method by PVP, which has been widely used as a surfactant for capping and a dispersing agent with its strong

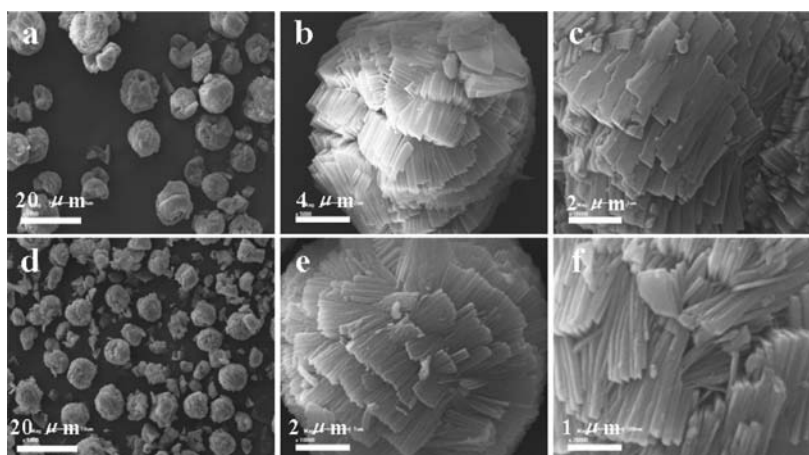
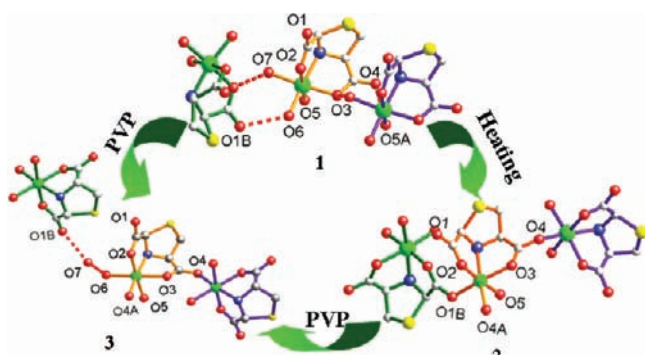


Figure 8. SEM images of 3 in the micrometer-particle form obtained at 25 (a, b, and c) and 80 °C (d, e, and f).

**Scheme 4. Schematic Representation of the Structure Conversions of Discrete 1, Left Helical Chain 3, and 3D Framework 2<sup>a</sup>**



<sup>a</sup>Color code: green, Ni; gray, C; red, O; blue, N; and red dot line for hydrogen bonds.

electrostatic and hydrogen bonding effects.<sup>16</sup> In this work, the hydrogen bonding interactions among PVP, water, and L as well as the interactions between PVP and Ni(II) ions could influence the process of coordination reactions strongly and result in the formation of the left-handed helical structure. Considering the same structure obtained at 25 and 80 °C for 3, the structure-directing force from the stimuli of PVP is stronger than that of temperature in this system.

Compared with the phenomena of form and structure conversions for Co(II) complexes reported by our group,<sup>12</sup> the series of Ni(II) complexes exhibit new features. For the Co(II) complexes, the molecular structures of two complexes exchange with each other together with the conversion from bulk to micrometer crystals when adding PVP into reaction systems, while for the Ni(II) complexes in this paper, molecular structures of both 1 and 2 are converted to the totally new one of 3 during the form conversions under the effect of PVP. Since the ligands and coordination configurations for Co(II) and Ni(II) complexes are the same, the different behavior of structure conversions could be attributed to the difference of Co(II) and Ni(II) ions on electronic configurations.

**Thermal Stability.** The thermogravimetric analyses (TGA) performed in the ambience indicate that the crystals are stable up to 278 °C for 1 and 3 and up to 298 °C for 2. Both 1 and 3 show a steady weight loss of water molecules below 144 °C, which can be assigned to the loss of three coordination water

molecules for 1 and one lattice water and two coordination waters for 3, respectively (observed, 15.8%; calculated, 17.1%). There was no further weight loss of those samples up to 273 °C. TGA of 2 shows two steps: one is a weight loss of 3.9% from 77 to 116 °C corresponding to the loss of half the lattice water molecules, and the other is a weight loss of 7.7% from 214 to 292 °C corresponding to the loss of the coordination water molecule. As shown in Figure 9, high stability and a

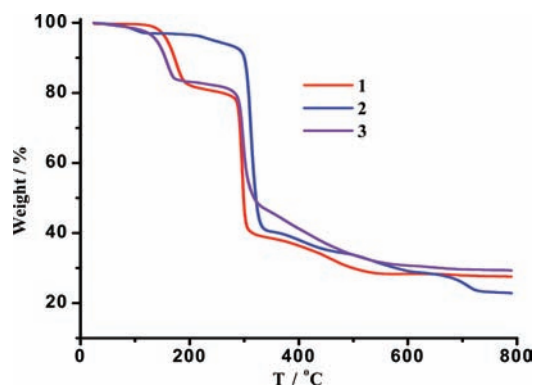


Figure 9. TGA curves for 1, 2, and 3.

similar trend for 1 and 3 can be attributed to the strong hydrogen bonding interactions among coordination water, lattice water, and the ligand.

**CD and NLO.** To examine the chiroptical and stable activities of the item products, the circular dichroism (CD) spectra of 1–3 in solid states were investigated. The CD spectra are shown in Figure 10; H<sub>2</sub>L gives rise to one positive band centered at 250 nm attributed to  $\pi \rightarrow \pi^*$  transitions. The bulk crystals of 1 and 2 as well as the micrometer-scale crystals of 3 exhibit one negative (250 nm) Cotton effect. These measurements further prove that the chirality of the ligand has been transferred to all of the [NiL]<sub>n</sub> aggregates. The non-centrosymmetric structure of the products prompted us to study NLO properties. Preliminary quasi-kurtz powder second-harmonic generation (SHG) measurements on the products exhibit modest SHG efficiencies approximately 0.5 (2) and 0.4 (3) times than that of urea.<sup>17</sup> All of these products are thermally robust and optically transparent, which indicates the potential application of them in practical NLO areas.

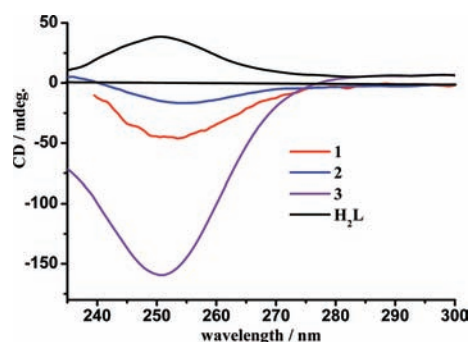


Figure 10. CD spectra of  $H_2L$ , **1**, **2**, and **3** in solid states.

## CONCLUSION

In summary, a series of bulk and micrometer-scale Ni(II)-containing chiral complexes have been designed and synthesized in different environments. Structure conversions of **1** to **2** and **1** and **2** to **3** associated with conformation changes have been observed and characterized by powder and single crystal X-ray diffraction. Notably, the structure conversions from **1** and **2** to **3** associated with the change of conformation of helical chains are triggered by the surfactant PVP. These results could lead to new methods for the research of chiral complexes in the areas of material and biology.

## EXPERIMENTAL SECTION

**Physical Measurements.** Analyses for C, H, and N were carried out on a Perkin-Elmer analyzer. Thermal gravimetric analyses were completed on a NETZSCH TG 209 instrument. CD experiments were performed on a Jasco J-715 spectropolarimeter at room temperature. The PXRD data were collected on a Rigaku D/max-2500 diffractometer with Cu K $\alpha$  radiation (40 kV and 100 mA). The single crystal XRD data were collected at 293(2) K on a Smart CCD area detector diffractometer with graphite-monochromated Mo K $\alpha$  radiation. The structure was solved by direct methods using SHELXS-97 and extended using Fourier techniques.

All chemicals were purchased from commercial sources and used without further purification. The ligand  $H_2L$  was prepared according to the literature method.<sup>13</sup>

**Synthesis of  $[NiL(H_2O)_3]$  (**1**).** In a typical experiment, an aqueous solution of  $Ni(CH_3COO)_2 \cdot 4H_2O$  (5.0 mL, 0.5 mmol) was added to thiazolidine 2,4-dicarboxylic acid (0.5 mmol) in 10.0 mL of water at room temperature (25 °C). The solution was mixed under vigorous stirring for 2 h at room temperature and then filtered. The filtrate was allowed to stand at room temperature. Green needle-like crystals of **1** were obtained after several days at room temperature. Elemental analysis (%) calcd for  $C_5H_{11}O_7SNNi$ : C, 20.86; H, 3.85; N, 4.86. Found: C, 20.73; H, 3.90; N, 4.83. IR (KBr,  $cm^{-1}$ ): 3415, 3287, 1619, 1559, 1428, 1384, 1278–524. The experimental procedure could be repeated easily with average yields of 35% (based on Ni).

**Synthesis of  $[NiL(H_2O)] \cdot 0.5H_2O$  (**2**).** In a typical experiment, an aqueous solution of  $Ni(CH_3COO)_2 \cdot 4H_2O$  (5.0 mL, 0.5 mmol) was added to thiazolidine 2,4-dicarboxylic acid (0.5 mmol) in 10.0 mL of water at 80 °C. The solution was mixed under vigorous stirring for 2 hours at 80 °C and then filtered. The filtrate was divided into three portions which were allowed to stand at room temperature. Green needle-like crystals of **2** were obtained after several days at room temperature. Elemental analysis (%) calcd for  $C_5H_8O_{5.5}SNNi$ : C, 23.02; H, 3.09; N, 5.37. Found: C, 22.86; H, 3.15; N, 5.33. IR (KBr,  $cm^{-1}$ ): 3415, 3287, 1619, 1559, 1428, 1384, 1278–524. The experimental procedure could be repeated easily with the average yields of 30% (based on Ni).

**Synthesis of Micrometer Particles of **3**.** A solution of  $Ni(CH_3COO)_2 \cdot 4H_2O$  (0.50 g, 2.00 mmol) in water was added to a PVP aqueous solution (11.2 g, 140.0 mL). After stirring for a few

minutes, an aqueous solution of thiazolidine 2,4-dicarboxylic acid (0.34 g, 2.00 mmol, 20.0 mL) was added to this solution at a certain temperature (25 or 80 °C). The obtained solution was mixed under vigorous stirring for 2 h at a certain temperature (25 or 80 °C). Afterward, it was left at a certain temperature (25 or 80 °C) overnight. The mixture was precipitated with 200.0 mL of acetone to yield a white suspension, which was isolated by centrifugation at 4000 rpm for 15 min. After removal of the supernatant, the particles were washed with ethanol (100 mL) several times. The ethanol suspension was centrifuged again for 15 min at 4000 rpm, and a light green powder was obtained in yields of 25% (at 25 °C) and 15% (at 80 °C; based on Ni), respectively. Bulk crystals of **3** with a conformation of  $\{[NiL(H_2O)_2] \cdot H_2O\}_n$  can be obtained by recrystallization of the nanoparticles from a water/methanol (v/v = 1:1) solution. Elemental analysis (%) calcd for  $C_5H_{11}O_7SNNi$  (**3**): C, 20.86; H, 3.85; N, 4.87. Found: C, 20.82; H, 3.89; N, 4.82).

Crystallographic data of complexes **1**, **2**, and **3** are found in Table 1.

Table 1. Crystallographic Data of Complexes **1**, **2**, and **3**

complexes	<b>1</b>	<b>2</b>	<b>3</b>
formula	$C_5H_{11}O_7SNNi$	$C_5H_8O_{5.5}SNNi$	$C_5H_{11}O_7SNNi$
mr	287.92	260.89	287.92
T (K)	293(2)	293(2)	293(2)
cryst syst	orthorhombic	tetragonal	monoclinic
space group	$P2_12_12_1$	$P4_1$	$P2_1$
a (Å)	5.8243	12.2986	5.3190
b (Å)	11.735	12.2986	9.5535
c (Å)	14.720	5.2444	9.7302
$\alpha$ (deg)	90	90	90
$\beta$ (deg)	90	90	101.23
$\gamma$ (deg)	90	90	90
V (Å <sup>3</sup> )	1006.1(3)	793.2(2)	484.97(17)
Z	4	4	2
$\rho$ (mg/cm <sup>3</sup> )	1.901	2.185	1.972
$\mu$ (mm <sup>-1</sup> )	2.152	2.704	2.232
F(000)	592	532	296
scan range $\theta$ (deg)	2.22–27.87	2.34–26.35	3.02–27.47
index ranges	$-7 \leq h \leq 7$	$-12 \leq h \leq 15$	$-6 \leq h \leq 6$
	$-14 \leq k \leq 15$	$-14 \leq k \leq 6$	$-12 \leq k \leq 12$
	$-19 \leq l \leq 19$	$-3 \leq l \leq 6$	$-12 \leq l \leq 12$
refln collected	2394	1265	2095
unique reflns	2206	1190	1982
$R_{int}$	0.0599	0.0233	0.0286
Flack factor	0.027(14)	0.018(19)	0.024(15)
data/restraints/ params	2394/0/139	1265/1/127	2095/1/138
GOF on $F^2$	1.064	1.010	1.013
$R_1, \omega R_2 [I > 2\sigma(I)]$	0.0333, 0.0617	0.0247, 0.0551	0.0295, 0.0583
$R_1, R_2$ (all data)	0.0383, 0.0637	0.0271, 0.0559	0.0328, 0.0602
largest diff. peak and hole (e.Å <sup>-3</sup> )	0.381, -0.571	0.274, -0.325	0.291, -0.530

## ASSOCIATED CONTENT

### Supporting Information

A crystallographic file in CIF format. This material is available free of charge via the Internet at <http://pubs.acs.org>.

## AUTHOR INFORMATION

### Corresponding Author

\*E-mail: [pcheng@nankai.edu.cn](mailto:pcheng@nankai.edu.cn).

### Notes

The authors declare no competing financial interest.



## ACKNOWLEDGMENTS

This work was supported by the 973 program (2012CB821702), NSFC (90922032 and 20971073) and MOE (IRT0927).

## REFERENCES

- (1) (a) Blaser, H. U. *Chem. Rev.* **1992**, *92*, 935–952. (b) Nandi, N.; Vollhardt, D. *Chem. Rev.* **2003**, *103*, 4033–4075. (c) Mellah, M.; Voituriez, A.; Schulz, E. *Chem. Rev.* **2007**, *107*, 5133–5209. (d) Yashima, E.; Maeda, K.; Nishimura, T. *Chem.—Eur. J.* **2004**, *10*, 42–51.
- (2) (a) Chen, H. M.; Zhang, J.; Bu, X. H. *Inorg. Chem.* **2009**, *48*, 6356–6358. (b) Seo, J. S.; Whang, D.; Lee, H.; Jun, S. I.; Oh, J.; Jeon, Y. J.; Kim, K. *Nature* **2000**, *404*, 982–986. (c) Meggers, E. *Chem.—Eur. J.* **2010**, *16*, 752–758. (d) Lorenzo, M. O.; Baddeley, C. J.; Muryn, C.; Raval, R. *Nature* **2000**, *404*, 376–379. (e) Orme, C. A.; Noy, A.; Wierzbicki, A.; McBride, M. T.; Grantham, M.; Teng, H. H.; Dove, P. M.; DeYoreo, J. J. *Nature* **2001**, *411*, 775–779.
- (3) Appelhans, L. N.; Kosa, M.; Radha, A. V.; Simoncic, P.; Navrotsky, A.; Parrinello, M.; Cheetham, A. K. *J. Am. Chem. Soc.* **2009**, *131*, 15375–15386.
- (4) (a) Zhang, J.; Chen, S. M.; Wu, T.; Feng, P. Y.; Bu, X. H. *J. Am. Chem. Soc.* **2008**, *130*, 12882–12883. (b) Lin, Z. J.; Slawin, A. M. Z.; Morris, R. E. *J. Am. Chem. Soc.* **2007**, *129*, 4880–4881.
- (5) Morris, R. E.; Bu, X. H. *Nat. Chem.* **2010**, *2*, 353–361.
- (6) (a) Lee, S. J.; Lin, W. B. *Acc. Chem. Res.* **2008**, *41*, 521–537. (b) Zheng, X.-D.; Lu, T.-B. *CrystEngComm* **2010**, *12*, 324–336.
- (7) Yuan, G. Z.; Zhu, C. F.; Liu, Y.; Xuan, W. M.; Cui, Y. *J. Am. Chem. Soc.* **2009**, *131*, 10452–10460.
- (8) Kamikawa, Y.; Nishii, M.; Kato, T. *Chem.—Eur. J.* **2004**, *10*, 5942–5951.
- (9) (a) Timoneda, M. A. M.; Calama, M. C.; Reinhoudt, D. N. *Chem.—Eur. J.* **2006**, *12*, 2630–2638. (b) Barberá, J.; Giorgini, L.; Paris, F.; Salatelli, E.; Tejedor, R. M.; Angiolini, L. *Chem.—Eur. J.* **2008**, *14*, 11209–11221. (d) Katzenelson, O.; Zabrodsky, H.; Hel-Or, H.; Avnir, D. *Chem.—Eur. J.* **1996**, *2*, 174–181. (e) García, L. P.; Amabilino, D. B. *Chem. Soc. Rev.* **2002**, *31*, 342–356.
- (10) (a) Mel'nikov, S. M.; Sergeyev, V. G.; Yoshikawa, K. *J. Am. Chem. Soc.* **1995**, *117*, 9951–9956. (b) Chu, D. Y.; Tomas, J. K. *J. Am. Chem. Soc.* **1986**, *108*, 6276–6289.
- (11) French, A. N. *Science* **2010**, *11* (328), 1365–1366. (b) Bradshaw, D.; Claridge, J. B.; Cussen, E. J.; Prior, T. J.; Rosseinsky, M. J. *Acc. Chem. Res.* **2005**, *38*, 273–282. (c) Corma, A.; García, H.; Xamena, F. X. L. *Chem. Rev.* **2010**, *110*, 4606–4655. (d) Chen, Y.; Ma, J.-G.; Zhang, J. J.; Shi, W.; Cheng, P.; Liao, D. Z.; Yan, S. P. *Chem. Commun.* **2010**, *46*, 2073–2075.
- (12) Yin, Y.-Y.; Chen, X.-Y.; Cao, X.-C.; Shi, W.; Cheng, P. *Chem. Commun.* **2012**, *48*, 705–707.
- (13) Refouvelet, B.; Robert, J. R.; Couquelet, J.; Tronche, P. *J. Heterocycl. Chem.* **1994**, *31*, 77–81.
- (14) Majeed, Z.; Mondal, K. C.; Kostakis, G. E.; Lan, Y. H.; Anson, C. E.; Powell, A. K. *Chem. Commun.* **2010**, *46*, 2551–2553.
- (15) (a) Zhao, B.; Chen, X.-Y.; Cheng, P.; Liao, D.-Z.; Yan, S.-P.; Jiang, Z.-H. *J. Am. Chem. Soc.* **2004**, *126*, 3012–3013. (b) Vittal, J. J.; Yang, X. D. *Cryst. Growth Des.* **2002**, *2*, 259–262. (c) Forster, P. M.; Burbank, A. R.; Livage, C.; Férey, G.; Cheetham, A. K. *Chem. Commun.* **2004**, 368–369. (d) Armentano, D.; Munno, G. D.; Mastropietro, T. F.; Julve, M.; Llore, F. *J. Am. Chem. Soc.* **2005**, *127*, 10778–10779. (e) Ranford, J. D.; Vittal, J. J.; Wu, D. Q. *Angew. Chem., Int. Ed.* **1998**, *37*, 1114–1116.
- (16) (a) Uemura, T.; Kitagawa, S. *J. Am. Chem. Soc.* **2003**, *125*, 7814–7815. (b) Zhang, Y. J.; Lu, J. J. *Cryst. Growth Des.* **2008**, *8*, 2102–2107. (c) Uemura, T.; Kitagawa, S. *Chem. Lett.* **2005**, *34*, 132–137.
- (17) Kurtz, S. K.; Perry, T. T. *J. Appl. Phys.* **1968**, *39*, 3798–3813.